

Clemastine Attenuates AD-like Pathology in an AD Model Mouse via Enhancing mTOR-Mediated Autophagy

Zhen-Yu Li

Soochow University

Li-Hua Chen

Soochow University

Xiu-Yun Zhao

Soochow University

Hong Chen

Soochow University

Mei-Hong Lu

Soochow University

Yan-Yun Sun

Soochow University

Zhao-Tao Wang

Soochow University

Mei Chen

Soochow University

Li Lu

Shanxi Medical University

Wenhui Huang

university of saarland

De-En Xu

Wuxi No.2 People's Hospital

Ru-Xiang Xu

university of Electronic Science and Technology of China

Quanhong Ma (✉ maquanhong@suda.edu.cn)


Soochow University <https://orcid.org/0000-0001-9392-8956>

Research

Keywords: clemastine, autophagy, mTOR, Alzheimer's disease, neurodegenerative disease

Posted Date: June 29th, 2020

DOI: <https://doi.org/10.21203/rs.3.rs-36989/v1>

License:  This work is licensed under a Creative Commons Attribution 4.0 International License.
[Read Full License](#)

Version of Record: A version of this preprint was published at Experimental Neurology on August 1st, 2021. See the published version at <https://doi.org/10.1016/j.expneurol.2021.113742>.

Abstract

Background: Alzheimer's disease (AD) is a neurodegenerative disorder with limited available drugs for treatment. Enhancing autophagy attenuates AD pathology in various AD model mice. Thus, development of potential drugs enhancing autophagy may bring beneficial effects in AD therapy.

Methods: In the present study, we showed clemastine, a first-generation histamine H1R antagonist and being originally marketed for the treatment of allergic rhinitis, ameliorates AD pathogenesis in APP/PS1 transgenic mice. Chronic treatment with clemastine orally reduced amyloid- β (A β) load, neuroinflammation and cognitive deficits of APP/PS1 transgenic mice as shown by immunohistochemistry and behavioral analysis. We further analyzed the mechanisms underlying the beneficial effects of clemastine with using the combination of both *in vivo* and *in vitro* experiments. We observed that clemastine decreased A β generation via reducing the levels of BACE1, CTFs of APP. Clemastine enhanced autophagy concomitant with a suppression of mTOR signaling.

Conclusion: Therefore, we propose that clemastine attenuates AD pathology via enhancing mTOR-mediated autophagy.

Introduction

Alzheimer's disease (AD) is a neurodegenerative disease characterized by deficits in learning, memory, and other cognitive functions. Its major pathological characteristics are the presence of amyloid- β (A β) plaques formed by accumulated A β and neurofibrillary tangles (NFTs) consisted of hyperphosphorylated tau (Lu et al., 2018). Although the pathological mechanisms of AD remain unclear, the accumulation of A β , which induces neuroinflammation and impaired synaptic plasticity, are believed as one of key initiators in AD pathogenesis (Lu et al., 2018;Uddin et al., 2018). Reducing accumulation of A β or suppressing neuroinflammation is a therapeutic strategy of AD. In this regard, autophagy has drawn great attention due to the following facts: Impaired autophagy has been extensively observed in the brains of AD patients and model mice. Enhancing autophagy attenuates AD pathology including the accumulation of A β , impaired synaptic plasticity and neuroinflammation (Hong et al., 2018;Liu and Li, 2019;Uddin et al., 2018;Wang et al., 2019;Wu et al., 2015). Thus, development of potential drugs enhancing autophagy may bring therapeutic effects on AD.

Clemastine (Tavegil™), a first-generation histamine H1R antagonist, is originally marketed for the treatment of allergic rhinitis. Clemastine contains several hydrophobic functional groups facilitating the crossing of the blood–brain barrier (BBB). Clemastine is currently on phase III clinical trial for patients with relapsing forms of multiple sclerosis due to its recently discovered remyelinating properties (Green et al., 2017;Li et al., 2015). Clemastine displays a beneficial effect in restoring spatial working memory in cuprizone-induced demyelinated mice (Li et al., 2015). Clemastine confers neuroprotection and induces an anti-inflammatory phenotype in SOD1G93A mouse model of amyotrophic lateral sclerosis (ALS) (Apolloni et al., 2016). Clemastine also exhibits a therapeutic effect in depression model mice via

modulating neuroinflammation and enhancing remyelination (Liu et al., 2016; Su et al., 2018). In summary, clemastine exhibits beneficial effects in various neurological disorders via conferring neuronal protection, attenuating neuroinflammation and enhancing remyelination, all of which related to AD pathology.

Herein, we investigated the potential therapeutic function of clemastine in AD using APP/PS1 transgenic mice, which harbor A β load, neuroinflammation and cognitive deficits, being extensively used in AD preclinical studies (Deng et al., 2016; Lu et al., 2018; Wang et al., 2019). APP/PS1 transgenic mice, which were treated orally with clemastine for 3 months from 4-month old of age, exhibited reduced load of A β plaques, neuroinflammation and improved cognitive function. Furthermore, clemastine decreased the levels of BACE1, α - and β -CTF of APP, the key enzyme cleaving APP to generate A β and the fragments of APP upon its cleavage at the extracellular domain respectively. Mechanismly, clemastine enhanced autophagy concomitant with a suppression of mTOR signaling. Our results indicate a potential therapeutic effect of clemastine in AD as an inducer of mTOR-mediated autophagy.

Materials And Methods

Animals

APP/PS1 transgenic mice (stock number 004462) were purchased from the Jackson Laboratory and maintained by breeding with C57BL/6 mice. Male APP/PS1 transgenic mice and the age-matched wildtype (WT) mice were used in all experiments.

Antibodies

Anti-A β (6E10, Convance, USA), anti-FL-APP (CST, USA), anti-APP C-terminal antibody (Sigma-Aldrich, USA), anti-BACE1 (Abcam, USA), anti-GFAP (Abcam), anti-Iba1 (Abcam), anti-mTOR (CST), anti-p-mTOR (CST), anti-P70S6K (CST), anti-p-P70S6K (CST), anti-LC3 (CST), anti-p62 (CST), anti-GAPDH (Sigma-Aldrich), anti-insulin degrading enzyme (IDE) (Santa Cruz, USA), anti-neprilysin (R&D, USA). Alexa Fluor-conjugated secondary antibodies were from Invitrogen. Horseradish peroxidase (HRP)-conjugated secondary antibodies were from Sigma-Aldrich.

Drug treatments

4-month old APP/PS1 transgenic mice and the age-matched WT mice were received a diet of standard laboratory chow supplemented with clemastine (10 mg/kg/day) (sodium salt; Tocris Bioscience, Bristol, Britain) for 4 months. The transgenic mice and WT mice received the same chow without clemastine.

Cell lines were treated with clemastine (dissolved in DMSO) at 0.3, 3, and 30 μ M for 12 h. Cells treated with DMSO served as control.

Cell culture and transfection

HeLa cells, HEK293 cells stably expressing human swedish mutant APP (HEK-APP), ATG5^{-/-} and ATG5^{-/-} MEFs cells were cultured in high glucose Dulbecco's Modified Eagle Medium supplemented with 10% fetal bovine serum (FBS) (Gibco, USA). Primary neurons were dissected from embryonic day (E) 17 APP/PS1 transgenic mice were cultured in neurobasal (Gibco) medium supplemented with 2% B27, 2 mM Glutamax-1 for 9-10 days. Lipofecamine 3000 (ThermoFisher, USA) was used for transfection according to the manufacturer's protocols.

Western blot analysis

The cultured cells were lysed with an SDS sample buffer (50 mM Tris-HCl (pH 6.8), 10% glycerol, 2% SDS, 0.1% bromophenol blue, and 6% 2-mercaptoethanol) for 10 min on ice. Lysates from the cortex and hippocampus were extracted in lysis buffer (50 mM Tris (pH 7.4), 150 mM NaCl, 1% TritonX-100, 1% sodium deoxycholate, 0.1% SDS) containing protease and phosphatase inhibitor cocktail (Roche, Switzerland). Lysates were subjected to SDS polyacrylamide gel electrophoresis, followed by transferring to a polyvinylidene fluoride membrane (Millipore, Darmstadt, Germany). The membrane was blocked in 5% BSA dissolved in Tris buffered saline containing Tween 20 (TBST) (20 mM Tris-HCL pH7.6, 150 mM NaCl, and 0.1% Tween 20) for 1 h at room temperature (RT), and then was incubated with appropriate antibody in 5% BSA diluted in TBST for overnight at 4°C. The membranes were washed with TBST and incubated with HRP-conjugated secondary antibodies (Sigma-Aldrich, USA) for 1 h at RT. The immunoreacted proteins were visualized using ECL Western Blotting Detection Reagents (Pierce, USA). The intensities of the bands were analyzed by Image J.

ELISA analysis

Human A β 42, A β 40 and levels were assessed by using sandwich ELISA. Frozen brain tissue was dissolved in TBS, and the soluble supernatant fractions were collected after centrifuged. The insoluble materials were then dissolved with Guanidine Hydrochloride. The soluble and insoluble A β were quantified using human A β 42 and A β 40 ELISA kits (KHB3441 and KHB3481, respectively; Invitrogen) following the manufacturer's instructions. The absorbance was read at 450 nm using a 96-well plate reader. A β levels were calculated from a standard curve and normalized to the total protein levels, which were determined by the BCA protein assay kit (ThermoFisher). All values were normalized to wet brain weight.

Immunofluorescence staining

Mice were perfused with phosphate-buffered saline (PBS), followed by 4 % paraformaldehyde at pH 7.4. Tissue samples were then postfixed overnight in 4 % paraformaldehyde and then cryoprotected in 30 % sucrose at 4 °C. Brain were cut in 12 μ m thickness with a frozen microtome. For immunofluorescence staining, sections were blocked in PBS containing 10% normal goat serum and 0.3 % Triton X-100 for 1 h at room temperature. Brain sections were incubated with primary antibody in blocking buffer overnight at 4°C. After rinsing in PBS, sections were incubated with appropriate secondary Alexa Fluor-conjugated antibodies for 2 h at RT. All sections were counterstained with 4, 6-diamidino-2-phenylindole (DAPI)

(Vector Laboratories) after being rinsed with PBS. Images were captured under a Leica confocal microscope.

HeLa cells line were fixed in 4% paraformaldehyde for 30 min on ice, followed by blocking in 10% FBS for 1 h at RT. The cells were then incubated with primary antibody in blocking buffer overnight at 4°C. After rinsing in PBS with 0.1% Triton X-100, cells were incubated with appropriate secondary Alexa Fluor conjugated antibodies for 1 h at RT. Images were captured under a Leica confocal microscope.

Image analysis

For quantification of GFP⁺ puncta, amyloid plaques, the densities of astrocytes and microglia, the images were converted into 8-bit images, and binarized after subtracting the background noise using Image J software. The numbers of GFP⁺ puncta per cell were counted; The density of A β plaques was expressed as the numbers of A β plaques per square micrometer; The size of A β plaques was quantified as the area that was occupied by A β plaques divided by total area of the cortex and hippocampus; That GFAP⁺ or Iba1⁺ signals divided by total area of the cortex and hippocampus was quantified as the volume of microglia and astrocytes respectively.

Morris water maze

Mice underwent 4 trials per day. A different starting position was used on each trial. The duration of one trial was 90 seconds. Escape latencies (time spent swimming from start point to the target) and path length (the distance from start point to the platform) before reaching the platform were recorded for 5 consecutive days. The escape latencies in the following training day were analyzed (escape latency in the following day/escape latency in the first day) and labeled as learning trend. For probe trials, the platform was removed after the last trial of the acquisition period. Mice were tested 24 hours later to assess memory consolidation. The time spent in the target quadrant within 60 seconds was recorded. The latency to the first target site was measured, and the numbers of platform-site crossovers were recorded.

Novel object recognition

Mice were exposed to 2 identical objects for 10 minutes placed in 2 opposite corners of the apparatus 8.5 cm from the sidewall. Ninety minutes after the training session, the animal explored the open field for 10 minutes in the presence of 1 familiar and 1 novel objects. Location preference = time exploring one of the identical objects/time exploring the identical object pairs \times 100%. Recognition index (RI) = time exploring novel object/ (time exploring novel object + time exploring familiar object) \times 100%.

Statistical analysis

All statistical analysis was performed using SPSS 20.0. Data were presented as mean \pm SEM. All dates were collected from at least three independent experiments or from three mice. Data between multiple groups were analyzed by one-way analysis of variance (ANOVA). Comparisons between two groups were

made by independent samples t-test. $P < 0.05$ was considered for the significance level for all analyses. *: $P < 0.05$; **: $P < 0.01$; ***: $P < 0.001$.

Results

Chronic clemastine treatment rescues cognitive deficits of APP/PS1 Transgenic Mice

We first examined whether clemastine might attenuate the cognitive deficits in APP/PS1 transgenic mice. APP/PS1 transgenic mice exhibit appearance of A β plaques from 3-month old. They develop AD-like pathology such as extensive A β plaques, neuroinflammation and cognitive deficits at 7-month old (Zhang et al., 2014). Thus, we have taken a prophylactic strategy as an early intervention in which four-month-old APP/PS1 transgenic mice were administered clemastine mixed in the food for 3 months. Clemastine exhibits beneficial effect in social isolation-caused depression model mice and in SOD1-G93A mice, a transgenic mouse model of amyotrophic lateral sclerosis (ALS) at 10 mg/kg/day (Apolloni et al., 2016). Thus, to prove the concept that whether clemastine might attenuate AD pathology, APP/PS1 mice were treated orally with clemastine at 10 mg/kg/day. APP/PS1 mice and age-matched WT mice fed with normal food were used as the control. In Morris water maze test, APP/PS1 mice showed impaired learning, as indicated by the increased escape latencies (Fig. 1A) and swimming distances (Fig. 1B, C) in the consecutive trials compared with WT mice. In contrast, clemastine-treated APP/PS1 mice showed shorter escape latencies (Fig. 1A), and decreased swimming distances (Fig. 1B, C) compared with control APP/PS1 mice, even to a level comparable to WT mice. In the probe trials, clemastine-treated APP/PS1 mice exhibited improved memory retention as indicated that they spent longer time in target quadrant (Fig. 1D) and swam to cross over the target site more times than control APP/PS1 mice (Fig. 1E), which are comparable to WT mice. The differences among these groups of mice were not due to the distinct swimming capability, since the swimming speed of these groups of mice was similar (Fig. 1F). In novel object recognition tests, no significant difference was observed in location preference during the training phase, indicating that the location of the objects does not affect the exploratory behavior of mice (Fig. 1H). In the testing phase, as demonstrated previously, control APP/PS1 mice displayed a reduced recognition index (RI) than WT mice, which was rescued by treatment with clemastine (Fig. 1H). It is noteworthy that clemastine treatment showed no effects on WT mice in the above-mentioned tests (Fig. 1A-H). These results indicate that the chronic treatment with clemastine rescues cognitive deficits in APP/PS1 mice.

Chronic clemastine treatment attenuates A β accumulation in APP/PS1 mice

Accumulation of A β is the central initiator of AD pathogenesis (Musiek and Holtzman, 2015). We thus examined whether clemastine treatment would decrease A β accumulation. The coronal section of the hippocampus and cortex of clemastine-treated APP/PS1 transgenic mice and the control mice were stained with an antibody against A β (6E10) (Fig. 2A, D). Results showed that the numbers (Fig. 2C, F) and size (Fig. 2B, E) of A β plaques were decreased in the hippocampus (Fig. 2A-C) and cortex (Fig. 2D-F) of clemastine-treated APP/PS1 transgenic mice, compared to that in control APP/PS1 transgenic mice.

These results indicate that chronic treatment with clemastine decreases the densities of A β plaques. We further examined whether the reduced densities of A β plaques were due to decreased A β concentrations in the brain. ELISA analysis showed that the levels of both soluble and insoluble A β 42 and A β 40 in the cortex and hippocampus of clemastine-treated APP/PS1 transgenic mice decreased, compared with those in control transgenic mice. These results indicate that chronic treatment with clemastine decreases accumulation of A β .

Chronic clemastine treatment attenuates neuroinflammation in APP/PS1 mice

Neuroinflammation is an essential contributor to the pathogenesis of AD. Microglia and astrocytes, the main types of cells in the inflammatory response in the central nervous system, are activated in the brains of AD patients and AD model mice (Calsolaro and Edison, 2016; Shadfar et al., 2015). Activated microglia and astrocytes accumulate around A β plaques and produce pro-inflammatory cytokines and chemokines, which cause synaptic dysfunction and neurodegeneration (Calsolaro and Edison, 2016). Anti-inflammatory therapy has therefore been credited as a strategy for reducing the risk or slowing the progression of AD (Shadfar et al., 2015). Clemastine has been reported to decrease microgliosis and expression of microglia-related inflammatory genes in the model mice of ALS (Apolloni et al., 2016). We thus examined whether clemastine treatment might also decrease neuroinflammation in APP/PS1 transgenic mice. The densities of astrocytes and microglia as indicated by the volume of GFAP⁺ (a marker for astrocytes, Fig. 3A, C) and Iba-1⁺ (a marker for microglia, Fig. 3B, D) cells decreased in both the hippocampus and the cortex of clemastine-treated APP/PS1 transgenic mice. These results indicate that chronic treatment with clemastine attenuates neuroinflammation in the brains of APP/PS1 transgenic mice.

Chronic clemastine treatment decreases β -amyloidosis of APP processing in vivo

Chronic treatment with clemastine decreases A β accumulation, neuroinflammation and cognitive deficits of APP/PS1 transgenic mice. Among these pathological processes, A β accumulation is the upstream cause (Musiek and Holtzman, 2015). We thus examined the mechanisms underlying that clemastine reduces A β accumulation. To further confirm that clemastine affects A β generation in neurons, primary cortical neurons derived from embryonic 17 days (E17) APP/PS1 transgenic mice were treated with clemastine. The result showed that A β 40 levels in culture medium were reduced by treatment with clemastine (Fig. 4A), confirming that clemastine can reduce A β levels in neurons, which is independent on glial cells. Moreover, the levels of neprilysin and insulin-degrading enzyme (IDE), two enzymes account for A β degradation, remained unchanged in the hippocampus and cortex of APP/PS1 transgenic mice upon treatment with clemastine (Fig. 4B-D), suggesting that clemastine may not being involved in A β clearance. Since the ratio of A β 40/A β 42, which can be altered by γ -secretase cleavage of APP (Borchelt et al., 1996), remained identical levels in between clemastine-treated and control APP/PS1 transgenic mice (Fig. 4K), indicating that clemastine treatment does not alter γ -secretase activity. We then examined the cleavage of APP by α -/ β -secretase. APP is cleaved by α - or β -secretase at the extracellular domain, generating two fragments called α - or β -CTF, respectively (Musiek and Holtzman, 2015). The

levels of both α - and β -CTF, but not full-length APP, were decreased in the hippocampus and cortex of clemastine-treated APP/PS1 transgenic mice, compared to that in control transgenic mice (Fig. 4E-H). β -CTF is produced from cleavage of APP by BACE1 (Yan, 2016;Yan et al., 2016). Consistently, treatment with clemastine decreased BACE1 levels in the hippocampus and cortex of APP/PS1 transgenic mice (Fig. 4I, 4J). These results indicate that chronic treatment with clemastine reduces A β generation through suppressing cleavage of APP, especially by BACE1.

Clemastine treatment induces ATG5-dependent autophagy

Autophagy is a highly conserved catabolic process in which proteins and organelles are engulfed in double-membraned vacuoles called autophagosomes and then transported to lysosomes for degradation. Autophagy plays broad functions in neurodegenerative disease (Nixon, 2013). Both α -/ β -CTFs and BACE1 are degraded through autophagy (Tian et al., 2013;Wu et al., 2015). Moreover, co-treatment with H1R antagonist astemizole and histamine induces autophagy (Jakhar et al., 2016), suggesting that histamine signaling is involved in autophagy induction. Thus, to investigate the underlying molecular mechanisms of therapeutic effects of clemastine in AD pathogenesis, we examined the effect of clemastine on autophagy. Microtubule-associated protein light chain 3 (LC3) was used as a marker of autophagy induction, because cytosolic LC3-I is processed to its lipidated LC3-II form upon autophagy induction. LC3-II then locates to newly forming autophagophores and subsequently be present in mature autophagosomes (Wu et al., 2015). Therefore, processing of LC3 and a punctuate LC3 pattern represent the formation of autophagosomes and autophagic responses. HeLa cells transfected with LC3-GFP were treated with either 30 μ M clemastine or DMSO. HeLa cells exhibited much more LC3-GFP⁺ puncta 12 h after clemastine treatment (Fig. 5A, 5B), indicating that clemastine induces formation of autophagosomes. In addition, treatment with clemastine increases LC3-II levels in a dose-dependent manner (Fig. 5C, 5D). The increasement of LC3-II by clemastine was further enhanced in presence of chloroquine, a lysosomal inhibitor which inhibits fusion of autophagosomes to lysosomes, indicating that the increasement of LC3-II by clemastine is due to an enhanced autophagic influx. Consistently, levels of P62, a substrate of autophagy, were decreased by clemastine dose-dependently (Fig. 5C, 5E). ATG5 is an initial factor in autophagy induction. We then examined whether clemastine induced autophagy in a way dependent on ATG5. ATG5^{+/+} and ATG5^{-/-} MEF cells were treated with clemastine. The results showed that, like in HeLa cells, clemastine treatment increased LC3-II levels (Fig. 5H, 5J), whereas decreasing P62 levels (Fig. 5H, 5J) indicating an enhanced autophagy influx. In contrast, clemastine failed to do so in ATG5^{-/-} MEF cells (Fig. 5H-5J), indicating that clemastine induces ATG5-dependent autophagy. Consistent with the fact that autophagy is impaired in AD (Nixon, 2013), APP/PS1 transgenic exhibited increased levels of LC3-II. In contrast, chronic treatment with clemastine increased LC3-II (Fig. 5K, 5M) while decreasing P62 levels (Fig. 5K, 5L), as it did in cultured cells. Therefore, these results indicate that clemastine enhances autophagy. However, clemastine failed to increase the LC3-II levels in WT mice, indicating clemastine enhances autophagy in a context-dependent manner.

Clemastine enhances autophagy via the mTOR pathway both in vivo and vitro

We further explored molecular mechanisms underlying that clemastine induces autophagy. Target of rapamycin (mTOR) signaling, when being suppressed, is one of central pathways in autophagy induction (Zhu et al., 2019). We thus examined first whether clemastine could affect mTOR signaling. HeLa cells treated with distinct concentrations of clemastine revealed that clemastine decreased levels of phosphorylated mTOR (p-mTOR, Ser2448) (Fig. 6A, B) and phosphorylated P70S6K (p-P70S6K) (Fig. 6A, 6C) in a dose-dependent manner. In contrast, the levels of total mTOR (Fig. 6A, 6D) and P70S6K (Fig. 6A, 6E) remained unchanged upon treatment with clemastine. Similar results were observed in clemastine-treated APP/PS1 transgenic mice. The levels of p-mTOR and p-P70S6K, but not total mTOR and P70S6K, were decreased in the hippocampus and cortex of clemastine-treated APP/PS1 transgenic mice, compared to control transgenic mice (Fig. 6F-6H). However, clemastine did not alter mTOR signaling in WT mice, suggesting that clemastine suppresses mTOR signaling in an environment-dependent manner. Thus, these results indicate that clemastine suppresses mTOR signaling, a central pathway inducing autophagy.

Discussion

In the present study, we demonstrate that chronic treatment with clemastine rescues cognitive deficits in APP/PS1 transgenic mice by reducing A β load and neuroinflammation. We further observe clemastine enhances autophagy concomitant with a suppression of mTOR signaling, which is one of the key negative regulators of autophagy. The present study describes a potential therapeutic role of clemastine in AD via enhancing mTOR-mediated autophagy.

Impaired autophagy has been observed in the brains of AD patients and of various AD model mice. Enhancing autophagy attenuates AD-like pathology such as A β accumulation, tau phosphorylation, neuroinflammation and synaptic loss (Cho et al., 2014;Liu and Li, 2019;Lu et al., 2018;Wang et al., 2019;Wu et al., 2015). We herein observe that clemastine enhances autophagy in an ATG5-dependent manner. Furthermore, clemastine suppresses mTOR signaling, which is a suppressor of autophagy, in both primary cultured neurons and the brains of APP/PS1 transgenic mice. These results suggest that clemastine enhances autophagy through suppressing mTOR signaling. Clemastine is a first-generation histamine H1R antagonist. These results are also consistent with the facts that other histamine H1R antagonists induce autophagy (Hu et al., 2012;Steele and Gandy, 2013), suggesting that the antihistamine effect may contribute to the clemastine-enhanced autophagy. However, it is worth noting that in addition to H1R, clemastine acts to antagonize five more other targets including the five muscarinic acetylcholine receptor subtypes (Chrm1-Chrm5) (Kubo et al., 1987). Especially, clemastine enhances myelination via antagonizing Chrm1 in oligodendrocyte progenitor cells (OPCs) rather than via other four Chrm subtypes (Chrm2-5) (Mei et al., 2016). Thus, it remains further investigation in future the molecular mechanisms underlying that clemastine induces autophagy and attenuates AD pathology.

Clemastine exhibits beneficial effects in neurological disorders via acting on distinct neural cells. Clemastine suppresses microglia-mediated neuroinflammation, enhances myelination and protects neuronal survival. Through these distinct cellular mechanisms, clemastine exhibits beneficial effects on

ALS, depression, anxiety and MS (Apolloni et al., 2016;Green et al., 2017;Li et al., 2015;Su et al., 2018). Consistent with these observations, we herein have observed that clemastine treatment attenuates accumulation of A β , neuroinflammation and synaptic loss. In this regard, since accumulation of A β is the key initiator of AD pathogenesis, the attenuated neuroinflammation and synaptic loss may be the secondary change caused by reduced A β . However, it is worth noting that clemastine enhances autophagy, which plays essential roles in neurodegenerative diseases via keeping cellular homeostasis in different types of cells. For example, microglial autophagy degrades A β and regulates the release of inflammatory cytokines (Cho et al., 2014). Defective astrocytic autophagy contributes to oxidative stress and neuroinflammation (Wang and Xu, 2020). Neuronal autophagy is involved in the production, clearance and releasing A β (Son et al., 2012). We have herein confirmed clemastine induces autophagy in neurons by suppressing mTOR signaling. This observation is consistent with the facts that clemastine decreases the levels of A β , α/β -CTFs and BACE1, all of which are substrates of autophagy (Son et al., 2012;Tian et al., 2013;Wu et al., 2015;Yang et al., 2017), and that the generation of A β by APP cleavage is occurred predominantly in neurons (Wu et al., 2015). However, we still cannot exclude the potential contribution of clemastine in glial cells to AD pathogenesis, considering the essential roles of glial autophagy in AD pathology (Cho et al., 2014;Wang and Xu, 2020). It requires further investigation that whether and how clemastine regulates microglia- and/or astrocytes-mediated neuroinflammation and their contribution to AD pathogenesis.

Limitation

Our present study has the following limitation: Although we have described that clemastine, as a novel autophagy inducer, decreases the levels of CTFs and BACE1, thus suppressing A β generation in neurons. We did not examine whether and how clemastine regulates glial cells in AD mouse brains. Clemastine is clinical drug used for the treatment of allergic rhinitis, which shows good bioavailability and pharmacokinetics (Schran et al., 1996). However, it still requires further investigation on the biodistribution and pharmacokinetic profile of clemastine in AD transgenic mice, especially the efficacy of clemastine across BBB. The present study just proves the concept that clemastine exhibits a potentiality in AD therapy. However, to confirm whether clemastine is a potential drug for AD therapy, we should perform more extensive analysis in future such as different doses, the period of treatment, even with different AD model mice.

Conclusion

Chronic treatment with clemastine attenuates AD pathology including accumulation of A β plaques, neuroinflammation and cognitive deficits. Clemastine reduces A β generation by decreasing the levels of CTFs and BACE1, all of which are autophagic substrates. Clemastine enhances autophagy via suppression of mTOR signaling, which is one of the key negative regulators of autophagy. Therefore, the present study describes a potential therapeutic role of clemastine in AD via enhancing mTOR-mediated

autophagy. Considering that clemastine is already widely used in the treatment of allergic rhinitis, the present study highlights that clemastine may be a drug candidate in AD therapy.

Abbreviations

AD: Alzheimer's disease; A β : amyloid- β ; ALS: amyotrophic lateral sclerosis; BBB: blood–brain barrier; DAPI: 4, 6-diamidino-2-phenylindole; FBS: fetal bovine serum; IDE: insulin-degrading enzyme; LC3: Microtubule-associated protein light chain 3; mTOR: Target of rapamycin; NFTs: neurofibrillary tangles; OPCs: oligodendrocyte progenitor cells; PBS: phosphate-buffered saline; RI: Recognition index; RT: room temperature; TBST: Tris buffered saline containing Tween 20

Abbreviations

AD: Alzheimer's disease; A β : amyloid- β ; ALS: amyotrophic lateral sclerosis; BBB: blood–brain barrier; DAPI: 4, 6-diamidino-2-phenylindole; FBS: fetal bovine serum; IDE: insulin-degrading enzyme; LC3: Microtubule-associated protein light chain 3; mTOR: Target of rapamycin; NFTs: neurofibrillary tangles; OPCs: oligodendrocyte progenitor cells; PBS: phosphate-buffered saline; RI: Recognition index; RT: room temperature; TBST: Tris buffered saline containing Tween 20

Declarations

Acknowledgments

Not applicable.

Authors' contributions

Li ZY, Chen LH, Zhao XY, Chen H, Xu DE, Lv MH and Wang ZT performed the experiments. Chen M performed the statistical analysis. Huang W, Xu RX and Ma QH designed the project and wrote the manuscript.

Funding

This work was supported by National Natural Science Foundation of China (81870897, 81901296, 81601111, 81671111, 81571061), Natural Science Foundation of Jiangsu Province (BK20181436), National Major Scientific and Technological Special Project for “Significant New Drugs Development” (2019zx09301102), the Suzhou Clinical Research Center of Neurological Disease (Szzx201503), translational medicine fund of WuXi municipal health commission (ZM010), Priority Academic Program Development of Jiangsu Higher Education Institution (PAPD), Jiangsu Provincial Medical Key Discipline Project (ZDXKB2016022) and Jiangsu Provincial Special Program of Medical Science (BL2014042), Jiangsu Key Laboratory of Translational Research and Therapy for Neuro-Psycho-Diseases (BM2013003). W.H. was supported by Deutsche Forschungsgemeinschaft DFG Sino-German joint

project (KI 503/14-1) and the European Commission EC-H2020 FET ProAct Neurofibres EC-H2020 FET ProAct Neurofibres.

Availability of data and materials

All data analyzed or generated during current study are included in this published article and available from the corresponding author on reasonable request.

Ethics approval and consent to participate

Animal care and surgical procedures were approved by the Institutional Animal Care and Use Committee of Soochow University in accordance with international laws.

Consent for publication

Not applicable.

Competing interests

The authors declare no competing financial interests.

Author details

¹Jiangsu Key Laboratory of Neuropsychiatric Diseases, Institute of Neuroscience, Soochow University, Suzhou, Jiangsu Province 215021, China. ²Department of Neurosurgery, Sichuan Academy of Medical Sciences and Sichuan Provincial People's Hospital, School of Medicine, University of Electronic Science and Technology of China, Chengdu 610072, Sichuan, China. ³Wuxi No. 2 People's Hospital, Wuxi, Jiangsu Province 214000, China. ⁴Institute of Health and Disease, Binzhou Medical University, Yantai, Shandong province 264003, China. ⁵Department of Anatomy, Shanxi Medical University, Taiyuan 030001, China. ⁶Molecular Physiology, Center for Integrative Physiology and Molecular Medicine (CIPMM), University of Saarland, D-66421 Homburg, Germany.

References

1. Apolloni S, Fabbriozio P, Parisi C, Amadio S, Volonte C. Clemastine Confers Neuroprotection and Induces an Anti-Inflammatory Phenotype in SOD1(G93A) Mouse Model of Amyotrophic Lateral Sclerosis. *Mol Neurobiol*. 2016;53:518–31. doi:10.1007/s12035-014-9019-8.
2. Borchelt DR, Thinakaran G, Eckman CB, Lee MK, Davenport F, et al. Familial Alzheimer's disease-linked presenilin 1 variants elevate Abeta1-42/1–40 ratio in vitro and in vivo. *Neuron*. 1996;17:1005–13. doi:10.1016/s0896-6273(00)80230-5.
3. Calsolaro V, Edison P. Neuroinflammation in Alzheimer's disease: Current evidence and future directions. *Alzheimers Dement*. 2016;12:719–32. doi:10.1016/j.jalz.2016.02.010.

4. Cho MH, Cho K, Kang HJ, Jeon EY, Kim HS, et al. Autophagy in microglia degrades extracellular beta-amyloid fibrils and regulates the NLRP3 inflammasome. *Autophagy*. 2014;10:1761–75. doi:10.4161/auto.29647.
5. 10.1038/npp.2015.164
Deng QS, Dong XY, Wu H, Wang W, Wang ZT, et al Disrupted-in-Schizophrenia-1 Attenuates Amyloid-beta Generation and Cognitive Deficits in APP/PS1 Transgenic Mice by Reduction of beta-Site APP-Cleaving Enzyme 1 Levels. *Neuropsychopharmacology* (2016) 41: 440–453. doi: 10.1038/npp.2015.164.
6. Green AJ, Gelfand JM, Cree BA, Bevan C, Boscardin WJ, et al. Clemastine fumarate as a remyelinating therapy for multiple sclerosis (ReBUILD): a randomised, controlled, double-blind, crossover trial. *Lancet*. 2017;390:2481–9. doi:10.1016/S0140-6736(17)32346-2.
7. Hong Y, Liu Y, Zhang G, Wu H, Hou Y. Progesterone suppresses Abeta42-induced neuroinflammation by enhancing autophagy in astrocytes. *Int Immunopharmacol*. 2018;54:336–43. doi:10.1016/j.intimp.2017.11.044.
8. Hu WW, Yang Y, Wang Z, Shen Z, Zhang XN, et al. H1-antihistamines induce vacuolation in astrocytes through macroautophagy. *Toxicol Appl Pharmacol*. 2012;260:115–23. doi:10.1016/j.taap.2012.01.020.
9. Jakhar R, Paul S, Bhardwaj M, Kang SC. Astemizole-Histamine induces Beclin-1-independent autophagy by targeting p53-dependent crosstalk between autophagy and apoptosis. *Cancer Lett*. 2016;372:89–100. doi:10.1016/j.canlet.2015.12.024.
10. Kubo N, Shirakawa O, Kuno T, Tanaka C. Antimuscarinic effects of antihistamines: quantitative evaluation by receptor-binding assay. *Jpn J Pharmacol*. 1987;43:277–82. doi:10.1254/jjp.43.277.
11. Li Z, He Y, Fan S, Sun B. Clemastine rescues behavioral changes and enhances remyelination in the cuprizone mouse model of demyelination. *Neurosci Bull*. 2015;31:617–25. doi:10.1007/s12264-015-1555-3.
12. Liu J, Dupree JL, Gacias M, Frawley R, Sikder T, et al. Clemastine Enhances Myelination in the Prefrontal Cortex and Rescues Behavioral Changes in Socially Isolated Mice. *J Neurosci*. 2016;36:957–62. doi:10.1523/JNEUROSCI.3608-15.2016.
13. Liu J, Li L. Targeting Autophagy for the Treatment of Alzheimer's Disease: Challenges and Opportunities. *Front Mol Neurosci*. 2019;12:203. doi:10.3389/fnmol.2019.00203.
14. Lu MH, Zhao XY, Yao PP, Xu DE, Ma QH. The Mitochondrion: A Potential Therapeutic Target for Alzheimer's Disease. *Neurosci Bull*. 2018;34:1127–30. doi:10.1007/s12264-018-0310-y.
15. Mei F, Lehmann-Horn K, Shen YA, Rankin KA, Stebbins KJ, et al. Accelerated remyelination during inflammatory demyelination prevents axonal loss and improves functional recovery. *Elife* (2016) 5. doi:10.7554/eLife.18246.
16. Musiek ES, Holtzman DM. Three dimensions of the amyloid hypothesis: time, space and 'wingmen'. *Nat Neurosci*. 2015;18:800–6. doi:10.1038/nn.4018.

17. Nixon RA. The role of autophagy in neurodegenerative disease. *Nat Med.* 2013;19:983–97. doi:10.1038/nm.3232.
18. Schran HF, Petryk L, Chang CT, O'connor R, Gelbert MB. The pharmacokinetics and bioavailability of clemastine and phenylpropanolamine in single-component and combination formulations. *J Clin Pharmacol.* 1996;36:911–22. doi:10.1002/j.1552-4604.1996.tb04758.x.
19. Shadfar S, Hwang CJ, Lim MS, Choi DY, Hong JT. Involvement of inflammation in Alzheimer's disease pathogenesis and therapeutic potential of anti-inflammatory agents. *Arch Pharm Res.* 2015;38:2106–19. doi:10.1007/s12272-015-0648-x.
20. Son JH, Shim JH, Kim KH, Ha JY, Han JY. Neuronal autophagy and neurodegenerative diseases. *Exp Mol Med.* 2012;44:89–98. doi:10.3858/emmm.2012.44.2.031.
21. Steele JW, Gandy S, Latrepirdine. (Dimebon(R)), a potential Alzheimer therapeutic, regulates autophagy and neuropathology in an Alzheimer mouse model. *Autophagy.* 2013;9:617–8. doi:10.4161/auto.23487.
22. Su WJ, Zhang T, Jiang CL, Wang W. Clemastine Alleviates Depressive-Like Behavior Through Reversing the Imbalance of Microglia-Related Pro-inflammatory State in Mouse Hippocampus. *Front Cell Neurosci.* 2018;12:412. doi:10.3389/fncel.2018.00412.
23. Tian Y, Chang JC, Fan EY, Flajolet M, Greengard P. Adaptor complex AP2/PICALM, through interaction with LC3, targets Alzheimer's APP-CTF for terminal degradation via autophagy. *Proc Natl Acad Sci U S A.* 2013;110:17071–6. doi:10.1073/pnas.1315110110.
24. Uddin MS, Stachowiak A, Mamun AA, Tzvetkov NT, Takeda S, et al. Autophagy and Alzheimer's Disease: From Molecular Mechanisms to Therapeutic Implications. *Front Aging Neurosci.* 2018;10:04. doi:10.3389/fnagi.2018.00004.
25. Wang JL, Xu CJ. Astrocytes autophagy in aging and neurodegenerative disorders. *Biomed Pharmacother.* 2020;122:109691. doi:10.1016/j.biopha.2019.109691.
26. Wang ZT, Lu MH, Zhang Y, Ji WL, Lei L, et al. Disrupted-in-schizophrenia-1 protects synaptic plasticity in a transgenic mouse model of Alzheimer's disease as a mitophagy receptor. *Aging Cell.* 2019;18:e12860. doi:10.1111/acer.12860.
27. Wu H, Lu MH, Wang W, Zhang MY, Zhu QQ, et al. Lamotrigine Reduces beta-Site AbetaPP-Cleaving Enzyme 1 Protein Levels Through Induction of Autophagy. *J Alzheimers Dis.* 2015;46:863–76. doi:10.3233/JAD-143162.
28. Yan R. Stepping closer to treating Alzheimer's disease patients with BACE1 inhibitor drugs. *Transl Neurodegener.* 2016;5:13. doi:10.1186/s40035-016-0061-5.
29. Yan R, Fan Q, Zhou J, Vassar R. Inhibiting BACE1 to reverse synaptic dysfunctions in Alzheimer's disease. *Neurosci Biobehav Rev.* 2016;65:326–40. doi:10.1016/j.neubiorev.2016.03.025.
30. Yang C, Cai CZ, Song JX, Tan JQ, Durairajan SSK, et al. NRBF2 is involved in the autophagic degradation process of APP-CTFs in Alzheimer disease models. *Autophagy.* 2017;13:2028–40. doi:10.1080/15548627.2017.1379633.

31. Zhang MY, Zheng CY, Zou MM, Zhu JW, Zhang Y, et al. Lamotrigine attenuates deficits in synaptic plasticity and accumulation of amyloid plaques in APP/PS1 transgenic mice. *Neurobiol Aging*. 2014;35:2713–25. doi:10.1016/j.neurobiolaging.2014.06.009.
32. Zhu JW, Zou MM, Li YF, Chen WJ, Liu JC, et al. Absence of TRIM32 Leads to Reduced GABAergic Interneuron Generation and Autism-like Behaviors in Mice via Suppressing mTOR Signaling. *Cereb Cortex*. 2019. doi:10.1093/cercor/bhz306.

Figures

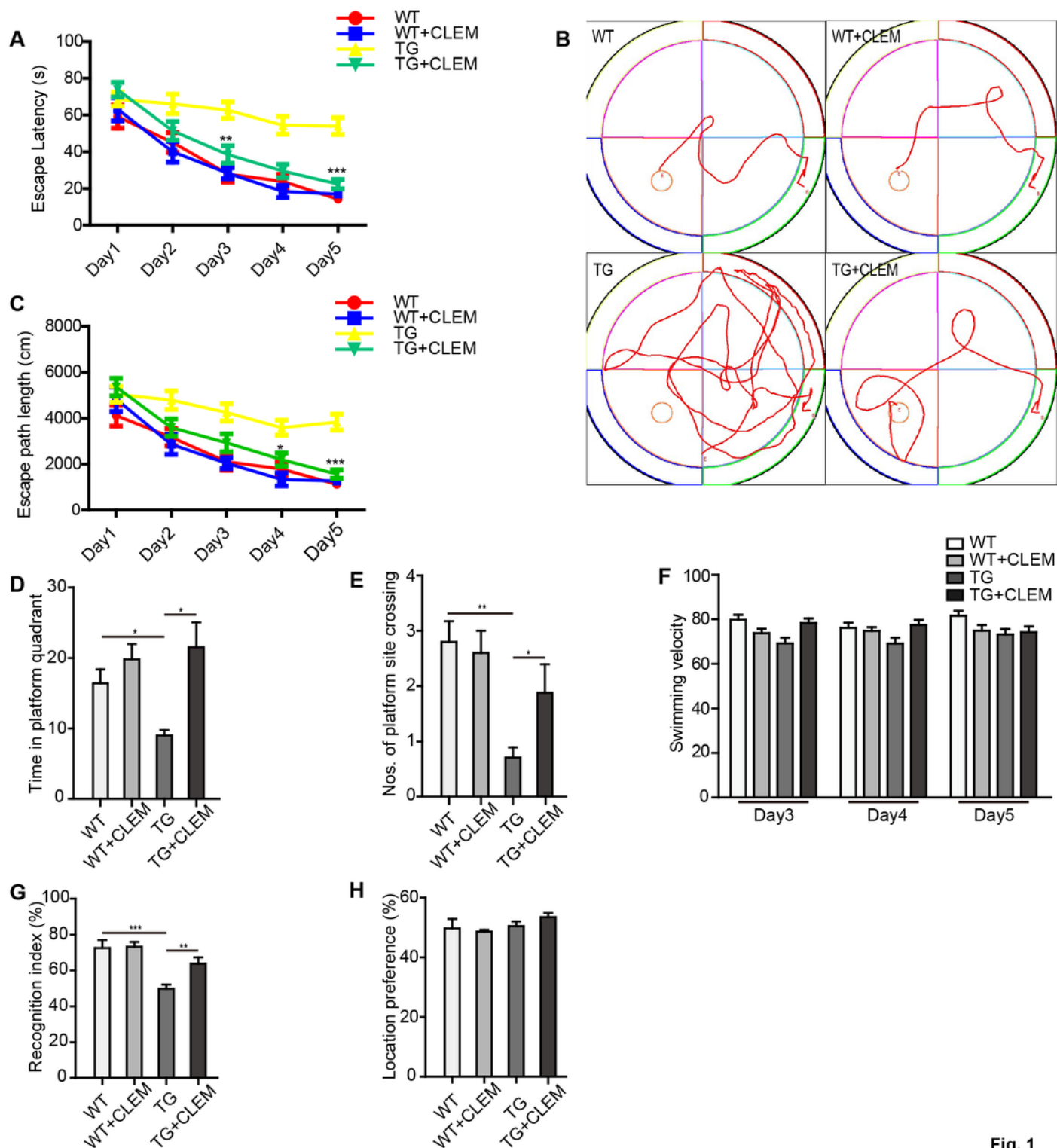


Fig. 1

Figure 1

Chronic clemastine treatment attenuates cognitive deficits of APP/PS1 mice. 4-month-old APP/PS1 transgenic mice were administered orally with clemastine (CLEM) for 4 months. The mice were then subjected to Morris water maze (A-F) and novel object recognition tests (G, H). (A) The escape latencies. (B) Representative images of the path that the mice swam along to find the platform. (C) The average distances that the mice spent to find the platform. (D) The time that the mice swam in the target platform

quadrant after retrieval of the platform. (E) The times that the mice swam across the target sites after retrieval of the platform. (F) Swimming speed. (G) Recognition index. (H) Location preference. Data are presented as mean \pm SEM. n=9-12 mice per group. * P< 0.05; ** P< 0.01. One-way ANOVA.

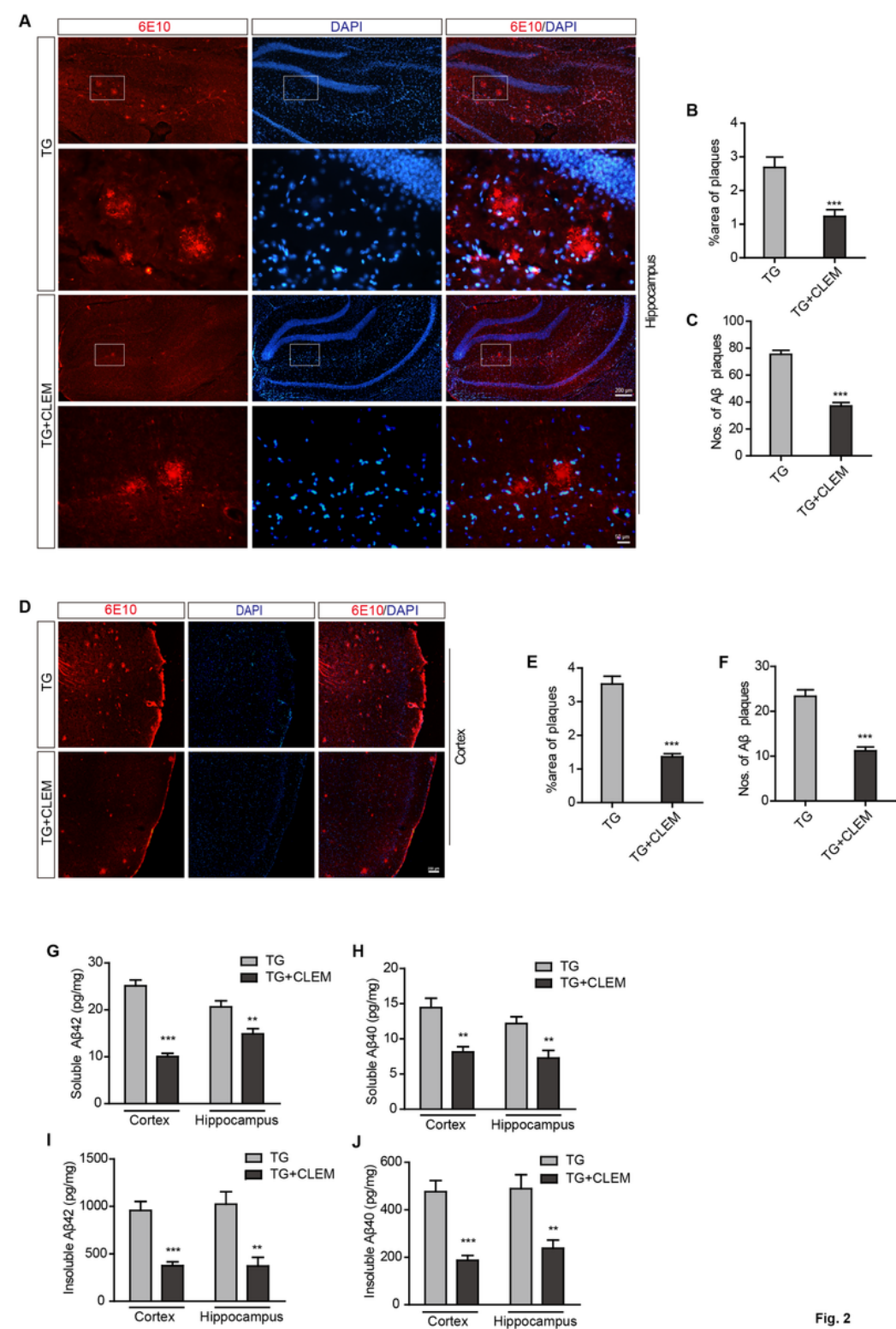


Fig. 2

Figure 2

Chronic clemastine treatment reduces Aβ generation in the brains of APP/PS1 mice. (A-F) The coronal sections of the hippocampus (A-C) and cortex (D-F) were stained with an antibody against Aβ (6E10).

Scale bars: 200 μ m and 50 μ m in images with higher magnification. The size of A β plaques in the hippocampus (B) and cortex (E) was quantified and expressed as the percentage of areas occupied by A β plaques. The numbers of A β plaques in the hippocampus (C) and cortex (F) were quantified and expressed as the amount of A β plaques per mm². (G-J) The levels of soluble (G, H) and insoluble (I, J) A β 40 (H, J) and A β 42 (G, I) in the cortex and hippocampus were analyzed by ELISA. Data are presented as mean \pm SEM. n=4 mice per group. *P< 0.05; **P< 0.01; ***P< 0.001. Independent samples t-test.

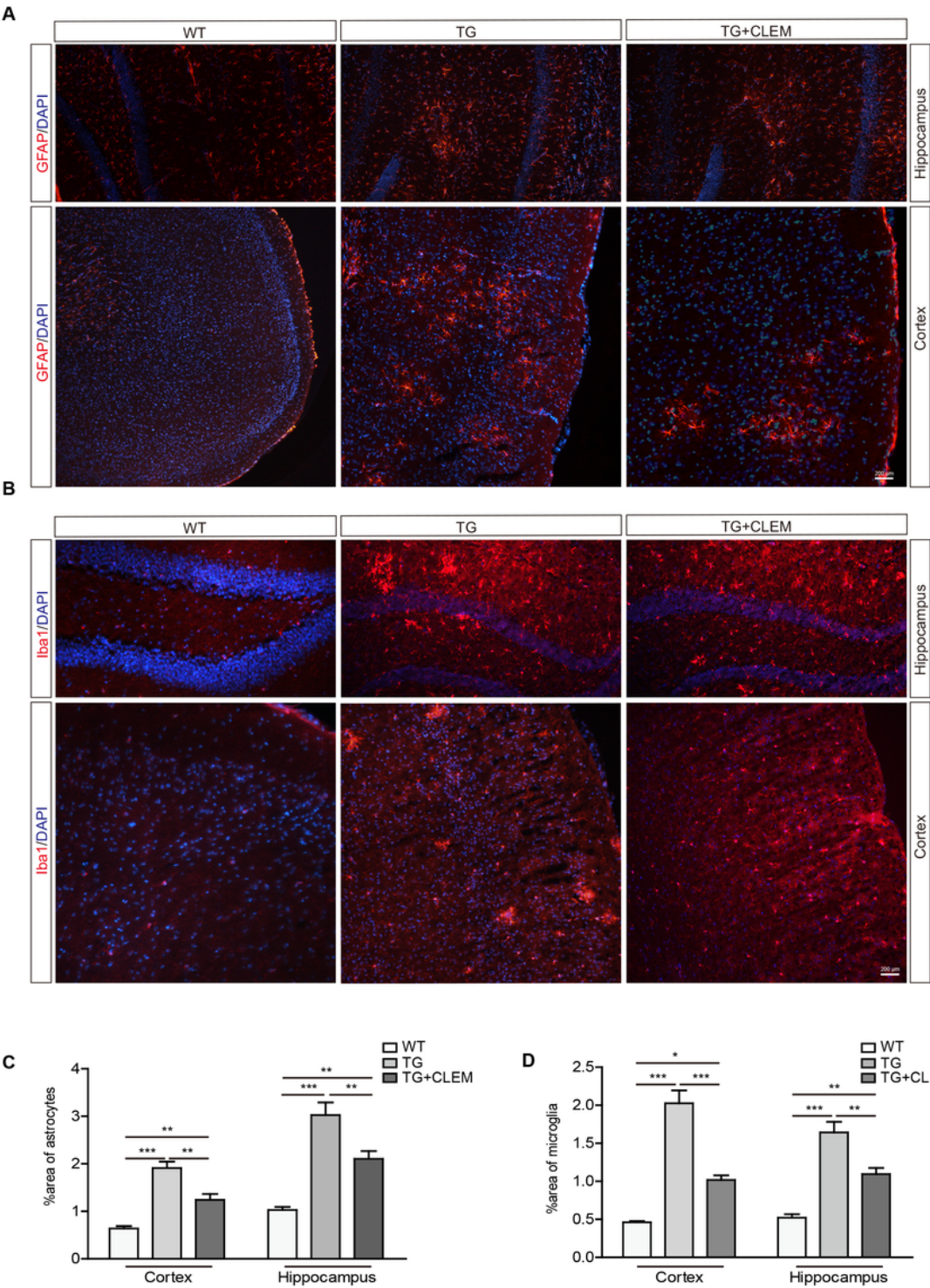


Fig. 3

Figure 3

Chronic clemastine treatment attenuates neuroinflammation in the brains of APP/PS1 mice. The coronal sections of the cortex and hippocampus were stained for GFAP (A) or Iba-1 (B) and DAPI. Scale bars: 200 μ m. (C) The percentage of the area of astrocytes (C) or Iba-1 (D) occupied in total area was quantified. (D) The percentage of the area of astrocytes occupied in total area in the frontal cortex and hippocampus was quantified. Data are presented as mean \pm SEM. n=4 mice per group. *P< 0.05; **P< 0.01; ***P< 0.01. One-way ANOVA.

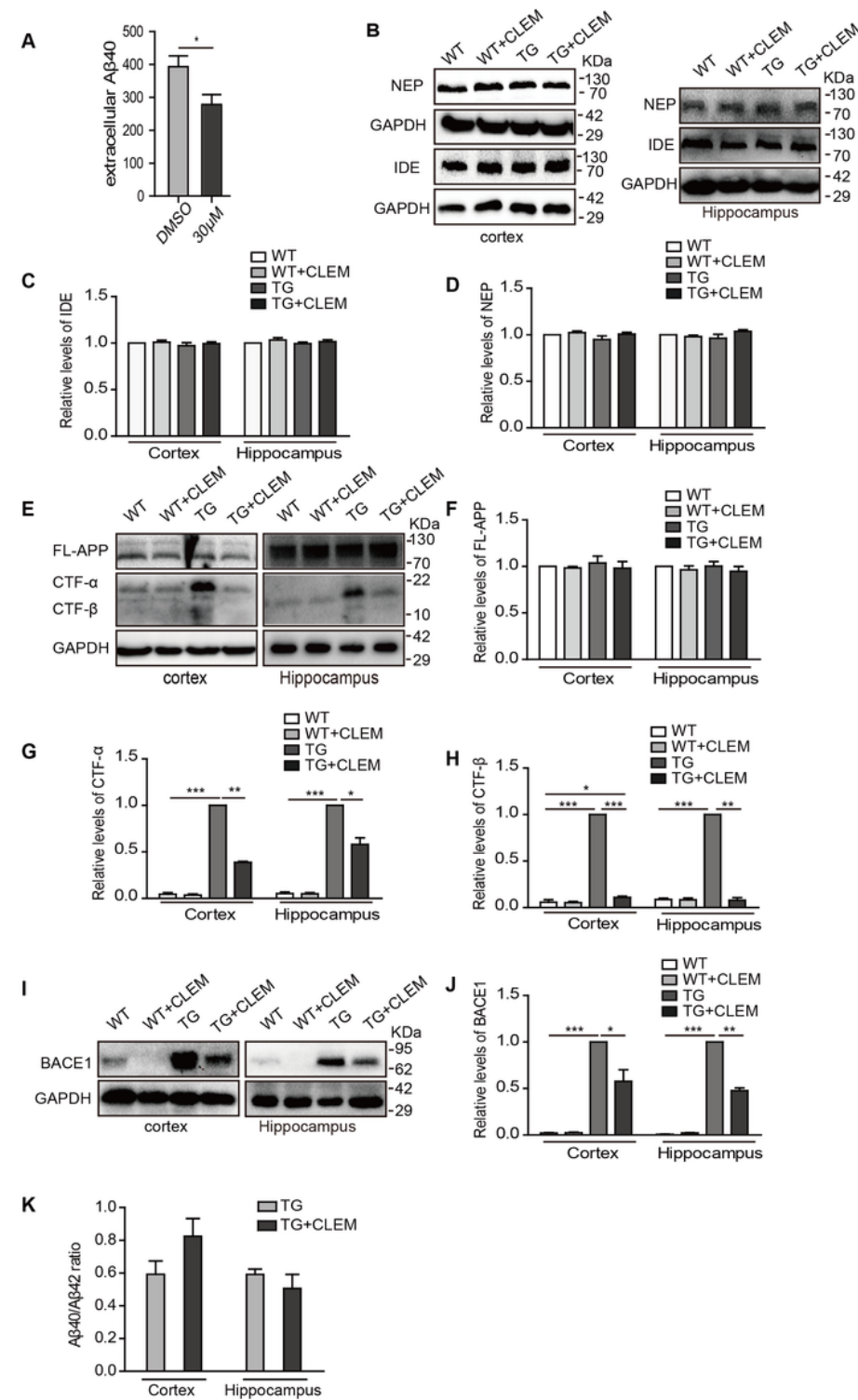


Fig.4

Figure 4

Chronic clemastine treatment decreases levels of BACE1 and α/β -CTFs in the brains of APP/PS1 mice. (A) ELISA analysis of levels of A β 40 in culture medium of primary neurons derived from E17 APP/PS1 mice. The relative levels of NEP (B, D), IDE (B, C), full-length APP (E, F), α - (E, G), β -CTF (E, H), BACE1 (I, J) and were analyzed by Western blotting and quantified. GAPDH as detected as loading control. (K) Analysis of the ratio of A β 40/A β 42. Data are presented as mean \pm SEM. n=4 mice per group. *P< 0.05; **P< 0.01; ***P< 0.01. One-way ANOVA.

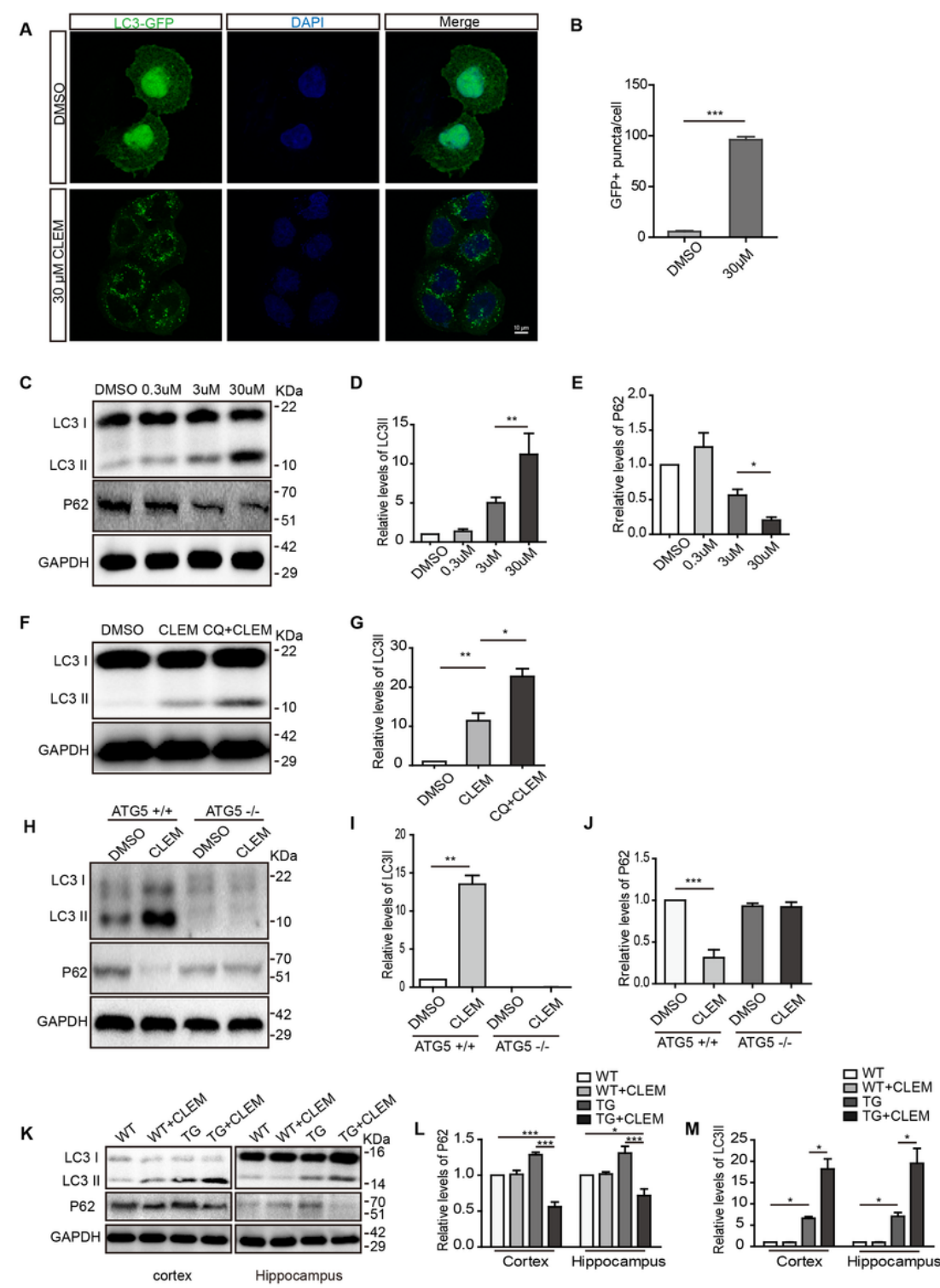


Fig.5

Figure 5

Clemastine induces Atg5-dependent autophagy. (A) HeLa cells transfected with GFP-LC3 were treated with 30 μ M clemastine for 12 h. (B) Numbers of GFP+ puncta were quantified. (C-E) HeLa cells were treated with 0.3 μ M, 3 μ M, 30 μ M clemastine for 12 h. Western blot analysis of levels of LC3-II (D), P62 (E). (F, G) HeLa cells were treated with chloroquine (CQ) and 30 μ M clemastine for 12 h. Western blot analysis of levels of LC3-I/II. (H-J) ATG5+/+ and ATG5-/- MEF cells were treated with 30 μ M clemastine for 12 h. Western blot analysis of levels of LC3-II (I) and P62 (J). (K-M) Western blot analysis of levels of LC3-I/II (M) or P62 (L) in APP/PS1 transgenic and their littermate WT mice, which were \were administrated with CLEM for 4 months. Data are presented as mean \pm SEM. n=3 independent biological repeats (A-J) or 4 mice per group (K-M). *P< 0.05; **P< 0.01; ***P< 0.01. Independent samples t-test (B) or One-way ANOVA (C-M).

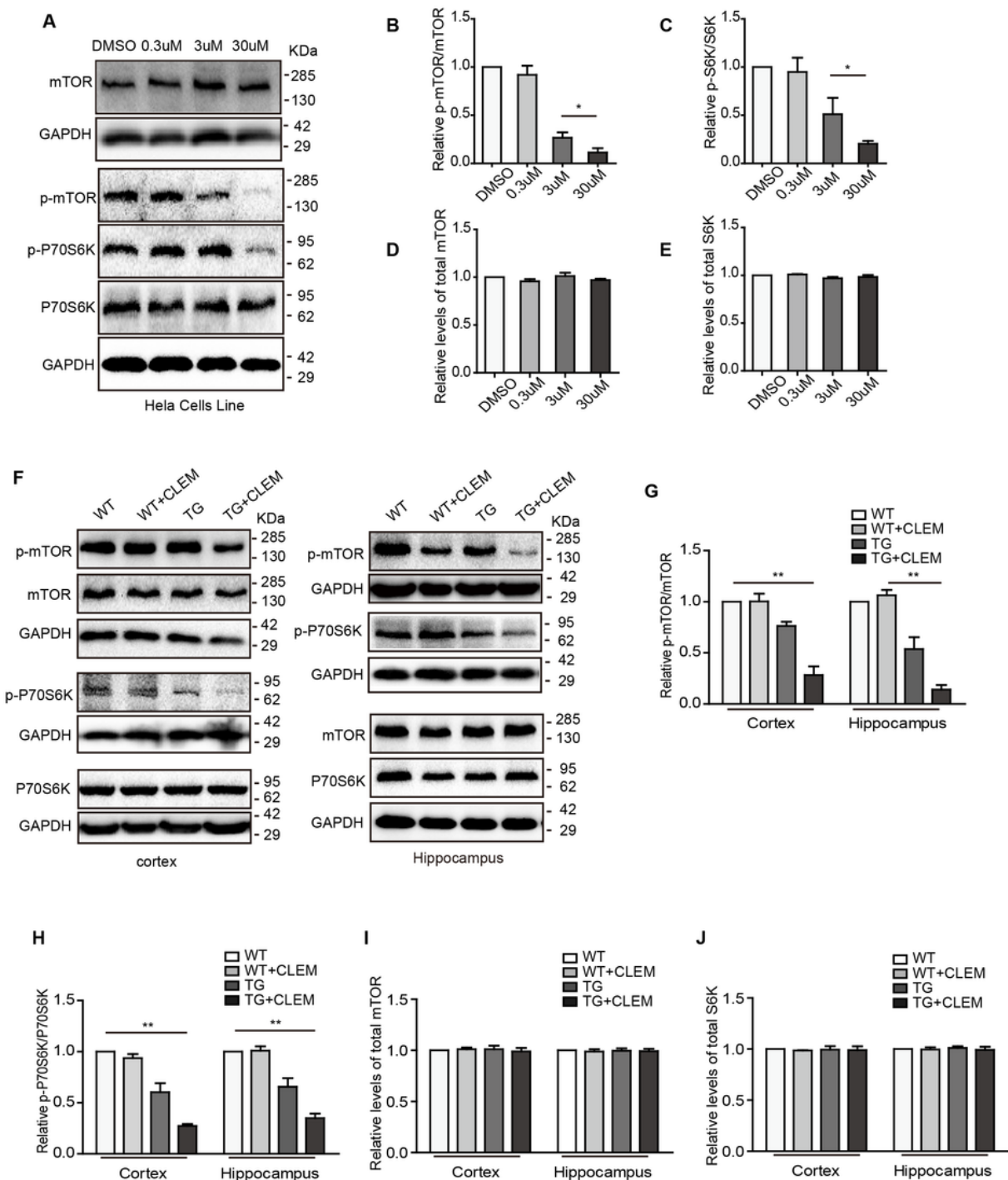


Fig. 6

Figure 6

Clemastine induces Atg5-dependent autophagy. (A) HeLa cells transfected with GFP-LC3 were treated with 30 μ M clemastine for 12 h. (B) Numbers of GFP+ puncta were quantified. (C-E) HeLa cells were treated with 0.3 μ M, 3 μ M, 30 μ M clemastine for 12 h. Western blot analysis of levels of LC3-II (D), P62 (E). (F, G) HeLa cells were treated with chloroquine (CQ) and 30 μ M clemastine for 12 h. Western blot analysis of levels of LC3-I/II. (H-J) ATG5^{+/+} and ATG5^{-/-} MEF cells were treated with 30 μ M clemastine

for 12 h. Western blot analysis of levels of LC3-II (I) and P62 (J). (K-M) Western blot analysis of levels of LC3-I/II (M) or P62 (L) in APP/PS1 transgenic and their littermate WT mice, which were \were administrated with CLEM for 4 months. Data are presented as mean \pm SEM. n=3 independent biological repeats (A-J) or 4 mice per group (K-M). *P< 0.05; **P< 0.01; ***P< 0.01. Independent samples t-test (B) or One-way ANOVA (C-M).